Jurnal Kejuruteraan 37(5) 2025: 2125-2136
https://doi.org/10.17576/jkukm-2025-37(5)-08

Structural, Morphological and Thermoelectric Characterization of CuO-ZnO Film Semiconductor for Thermoelectric Cell by Electrodeposition Method

Assayidatul Laila Nor Hairin[a*], Nurul Batrisyia Yusaini[a], Raihan Othman[b], Radhiyah Abd Aziz[c] & Mohd Faiz Mohd Salleh[d]

[a]*Department of Manufacturing and Materials Engineering, Kulliyah of Engineering, International Islamic University Malaysia, Malaysia.*

[b]*Department of Science in Engineering, Faculty of Engineering, International Islamic University Malaysia.*

[c]*Department of Mechanical Engineering,Faculty of Engineering, University Malaysia Pahang Al-Sultan Abdullah.*

[d]*Department of Electrical Engineering, Faculty of Engineering, University Malaya.*

[*]*Corresponding author: assayidatul_laila@iium.edu.my*

Received 4 October 2024, Received in revised form 9 April 2025
Accepted 9 May 2025, Available online 30 August 2025

ABSTRACT

Copper oxide (p-type CuO) and zinc oxide (n-type ZnO) thin film semiconductors were synthesized and evaluated as low-cost, environmentally friendly materials for a proof-of-concept thermoelectric device. The fabrication process involved alkaline vapor oxidation for CuO and a combination of electrodeposition and chemical bath deposition for ZnO, offering scalable and energy-efficient routes. The influence of NaOH concentration (3M, 4M, 5M) on CuO film properties was systematically studied. X-ray diffraction (XRD) and scanning electron microscopy (SEM) analyses revealed that films synthesized in 5M NaOH exhibited enhanced crystallinity and surface morphology. Alkaline vapor oxidation was conducted for 24 and 48 hours, and both CuO and ZnO films were subjected to thermoelectric characterization. Using a custom-built setup, Seebeck coefficient, electrical conductivity, and thermoelectric power factor (PF) were measured. The highest PF values were observed for ZnO (2.310 nW/K²·m) and CuO oxidized for 48 hours (2.746 nW/K²·m). These values align with reported ranges in recent literature and demonstrate the potential of CuO–ZnO systems in all-oxide thermoelectric generators. The results confirm that simple chemical processing routes can produce oxide thin films with viable thermoelectric performance, supporting sustainable and cost-efficient device fabrication. Furthermore, the morphological tuning through oxidation duration and concentration offers a pathway for material property engineering without requiring high-vacuum or high-temperature conditions. This study highlights the feasibility of integrating CuO and ZnO as a p–n junction pair in micro-scale or flexible energy recovery modules, particularly for wearable electronics or self-powered sensors operating in ambient or low-heat environments. The favorable material compatibility, low toxicity, and mechanical stability of the films also make them attractive candidates for next-generation energy harvesting technologies in distributed and low-power applications.

Keywords: p-type CuO; n-type ZnO; Seebeck coefficients; power factor (PF); electrodeposition

INTRODUCTION

Thermoelectric materials are a promising form of green technology that we need to agree because it can minimize the energy demand in relation to its ability to recycle the unused heat (Xiong et al. 2013). For example, conventional generators create electricity by burning the fuel, but the thermoelectric technology is more appealing approach to preserve the environment because it reuses the waste heat from the industry and auomotive sector (Shuai et al. 2017). Thermoelectric materials are compatible with any applications because they have no moving parts, create no noises, compact and have ability to operate for long term with minimum maintenance (Zlatic et al. 2012). Thermoelectric materials can be characterized by knowing the dimensionles figure-of-merit (ZT) where it is composed of three key properties, which are Seebeck coefficient (α), electrical conductivity (σ) and thermal conductivity (κ). The combined variable, , is usually called the thermoelectric power factor (TPF);

$$ZT = \alpha^2 \sigma T / \kappa \quad (1)$$

The ZT value can be improved by negotiating with the α, σ and κ (Su et al. 2011). Among the thermoelectric materials, p-type CuO and n-type ZnO semiconductors were chosen as thermoelectric materials has much interested due to its non-toxic, abundance, balance of desirable properties, cost-effectiveness, and ease of fabrication. Ongoing research and development efforts focus on improving the thermoelectric performance of CuO-ZnO by exploring novel nanostructuring approaches, advanced doping strategies, and composite material systems (Sulaiman et al. 2022). Due to their high degree of crystallinity, metal oxides have exceptional thermal stability at high temperatures and outstanding electrical conductivity. These characteristics will cause the material to improve thermoelectric power factor (TPF), which will allow the creation of TE devices with high efficiency and high temperature. According to literature (Zappa et al. 2014), highest TPF for p-type CuO and n-type ZnO semiconductors are 369.8 nW/(mK^2) and 8.1 nW/(mK^2) respectively. There are variety of method to synthesis p-CuO and n-ZnO including PVD, CVD, thermal oxidation, electrodeposition and etc. In this work, we present the fabrication by simple and low-cost physical methods of both p-CuO and n-type ZnO samples by using alkaline vapor oxidation, electrodeposition and chemical bath deposition methods.

METHODOLOGY

EXPERIMENTAL PROCEDURES

To synthesize the sample, first p-type CuO and n-type ZnO thin film have been fabricated independently in order to evaluate their intrinsic and individual thermoelectric properties. CuO were fabricated by alkaline vapor oxidation method (Soejima et al. 2013). It was done while ZnO were synthesized by electrodeposition and chemical bath deposition technique (Nkrumah et al. 2013).

Firstly, copper PCB substrates and acrylic holder were fabricate before the substrates were deposited by p-type CuO and n-type ZnO thin film. Figure 1 shows the copper PCB design and dimension used in this experiment. Four samples of p-type CuO thin film were deposited onto the copper pcb substrate by using different molarity of NaOH which were 3M, 4M for 24 hours and 5M for 24 and 48 hours at 60 □. Then, n-type ZnO thin film was fabricate by electrodeposit zinc onto the copper PCB substrate by using zinc foil which act as the anode and its electrolyte (and immersed it in the 1M NaOH solution which was concentrated with zinc oxide powder for one day. All these five samples were characterized by using SEM and XRD to identify its morphology and elements present.

Three samples were prepared which were p-type CuO

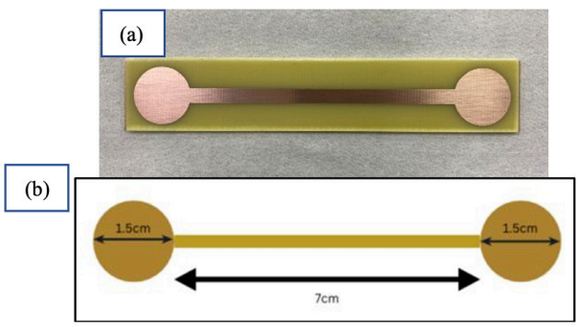

FIGURE 1. (a) Real figure of PCB substrate and
(b) illustration design and dimension of the copper PCB substrates.

that oxidized by 5M NaOH for 24 and 48 hours as well as n-type ZnO to undergo thermoelectric characterization. Seebeck coefficient and the electrical conductivity of the samples were determined by temperature gradient–voltage experiment and current-voltage experiment respectively. Seebeck coefficient and electrical conductivity were determined for all three samples by using a custom experimental set-up as in Figure 2. Lastly, the PF of each sample can be calculated by using the Seebeck coefficient and electrical conductivity values obtained.

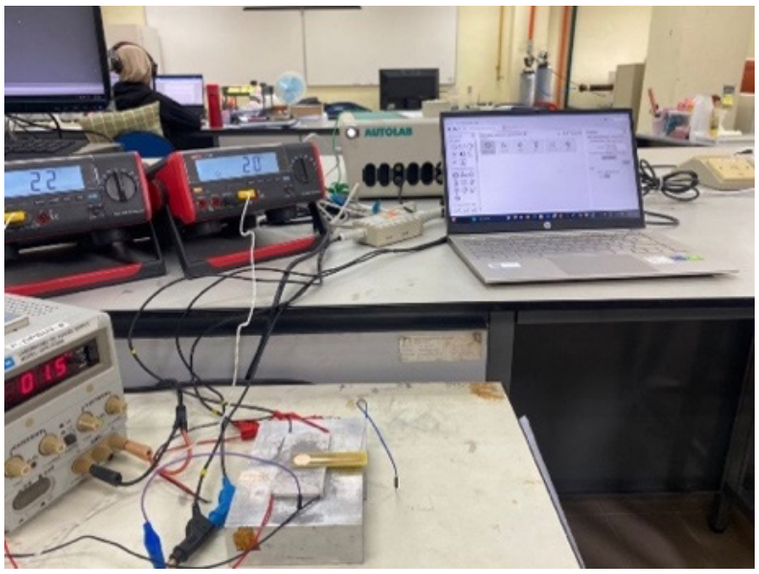

FIGURE 2. Custom experimental set up to determine the Seebeck coeficient and electrical conductivity of the samples.

RESULTS AND DISCUSSION

PHYSICAL PROPERTIES CHARACTERIZATION

COPPER OXIDE DEPOSITION IMAGE

The experiment was conducted to determine the homogenous distribution of p-type CuO on a copper substrate. Figure 3 shows that 5M NaOH can uniformly distribute p-type CuO onto the substrate. The concentration of NaOH affects the stability of the dispersion of p-type CuO particles in the solution. Higher NaOH concentrations can enhance the stability of the dispersion, preventing particle settling or agglomeration during the deposition process. This results in improved electrical and thermal transport properties, leading to enhanced thermoelectric performance.

ZINC AND ZINC OXIDE DEPOSITION

The deposited Zn can be seen on the copper substrate using naked eyes as it appeared in silver like color. Figure 4 shows the deposited Zn thin film on the copper substrate. After zinc was deposited, zinc oxide will be deposited by chemical bath deposition. The sample appear white after the process which indicates n-typeZnO layer.

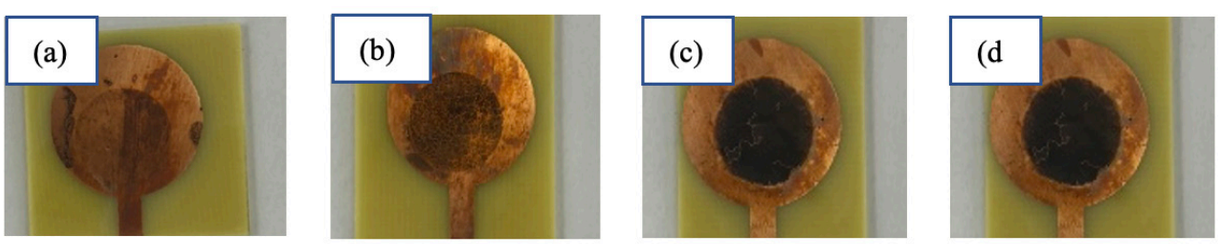

FIGURE 3. Deposition of CuO on Cu substrate by using (a) 3M NaOH, (b) 4M NaOH, (c) 5M NaOH for 24 hours and (d) 5M NaOH for 48 hours.

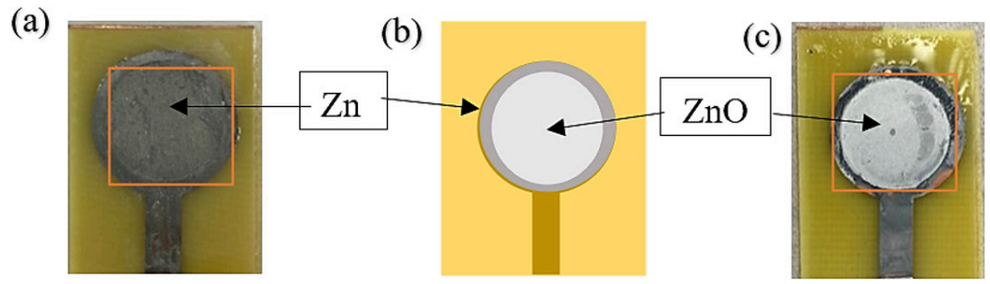

FIGURE 4. The real image of the zinc deposited on the copper substrate. (b) The illustration image of the deposited zinc and zin oxide on the copper substrate. (c) The real image of the zinc oxide deposited on the copper substrate.

SCANNING ELECTRON MICROSCOPY (SEM) ANALYSIS

1. COPPER OXIDE

Figure 5 show the surface morphology of the samples for CuO at magnification of x1000, x3000 and x5000 and the surface morphology of copper pcb substrate as a reference. To be compared copper structure that oxidized by 5M NaOH in Figure 7 can grow copper homogenously on the substrate while copper substrate still can be seen in Figure 5 and 6 when oxidized by 3M and 4M NaOH. Figure 8 highlight the structure of p-type CuO oxidized by 5M NaOH for 48 hours that can be observed has quiet high degree of vertical alignment compared to surface that was oxidized by 5M for 24 hours in Figure 7.

The thickness of copper oxide layer can be observed under SEM with magnification of x550. Figure 9 shows the thickness for copper oxide layer which has been oxidized with 5M NaOH for both 24 and 48 hours. The comparison in Figure 9 shows that the copper oxide layer that was oxidized for 48 hours is almost three times thicker than copper oxide layer which was oxidized by 24 hours.

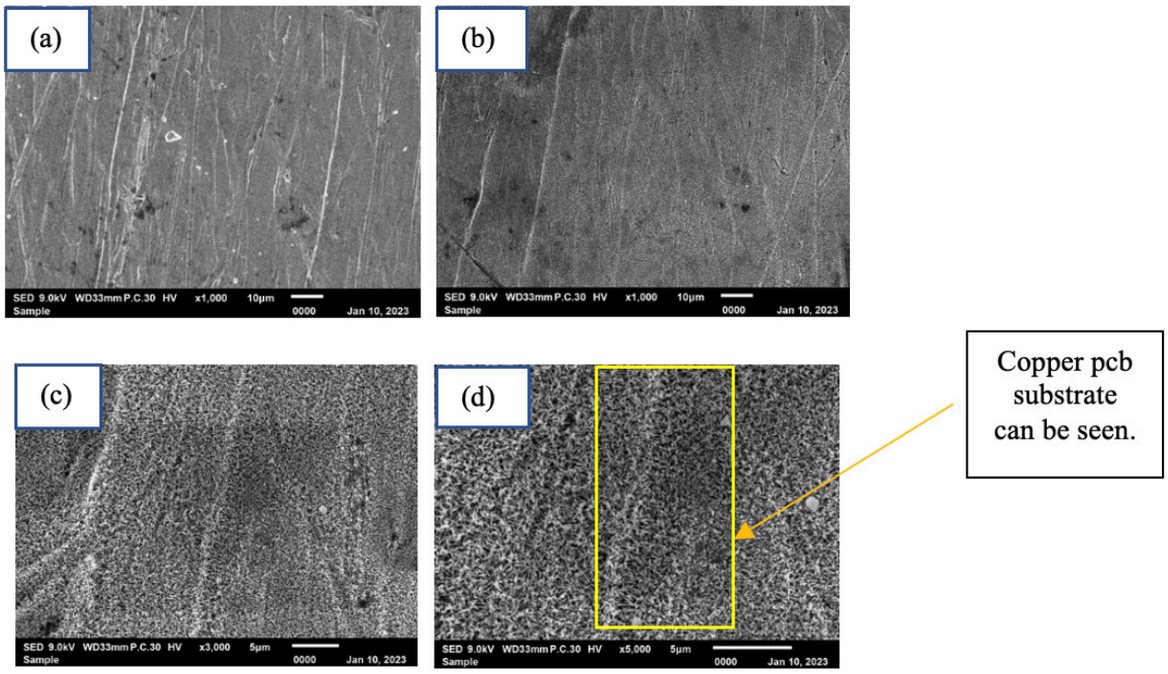

FIGURE 5. SEM characterization of (a) copper PCB and copper oxide oxidized by 3M NaOH solution for 24 hours with magnification of b) x1000, c) x3000, and d) x5000 respectively

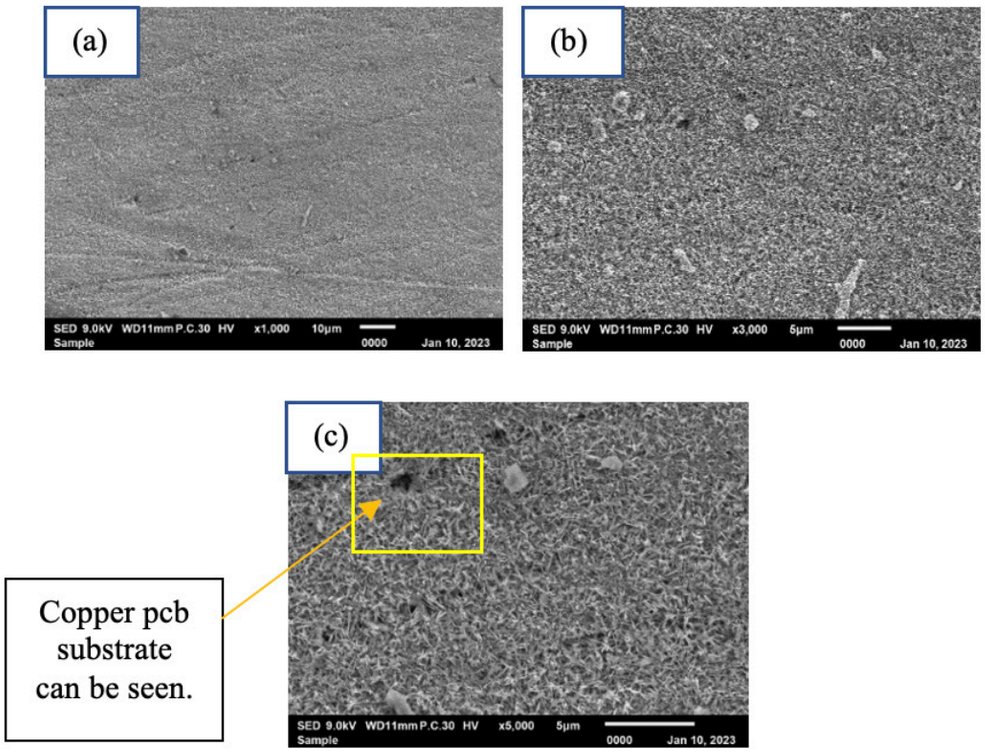

FIGURE 6. SEM characterization of copper oxide oxidized by 4M NaOH solution for 24 hours with magnification of a) x1000, b) x3000, and c) x5000 respectively

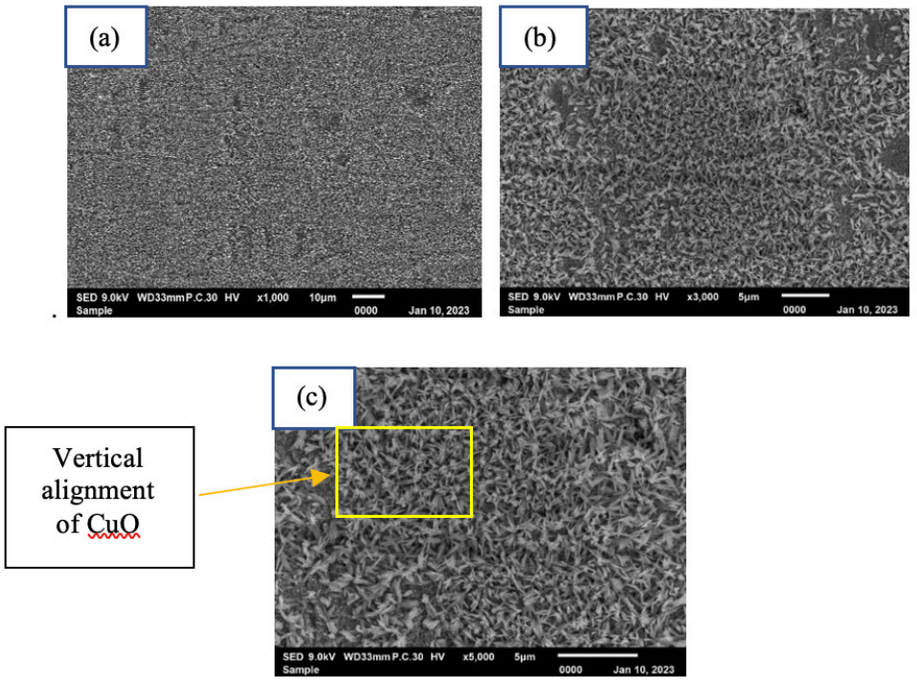

FIGURE 7. SEM characterization of copper oxide oxidized by 5M NaOH solution for 24 hours with magnification of a) x1000, b) x3000, and c) x5000 respectively

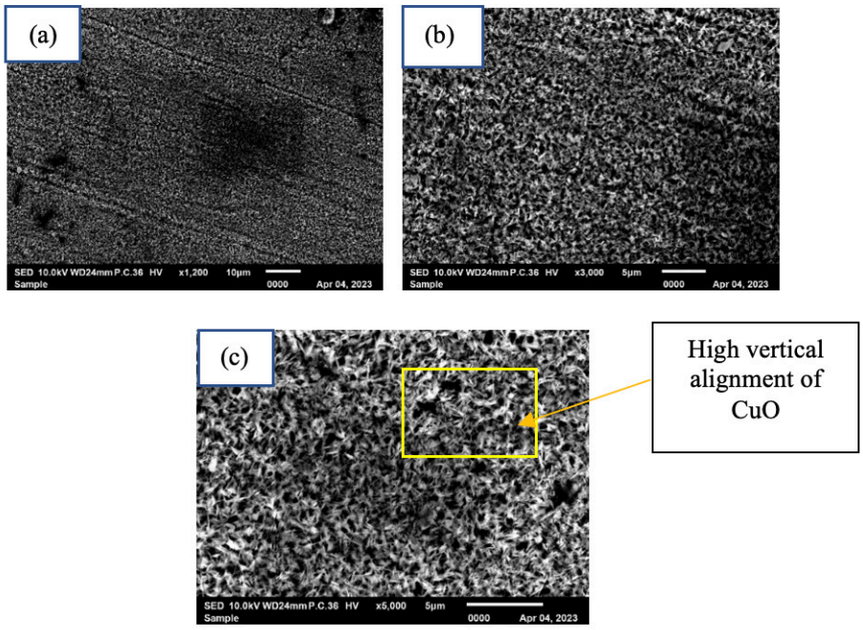

FIGURE 8. SEM characterization of copper oxide oxidized by 5M NaOH solution for 48 hours with magnification of a) x1000, b) x3000, and c) x5000 respectively

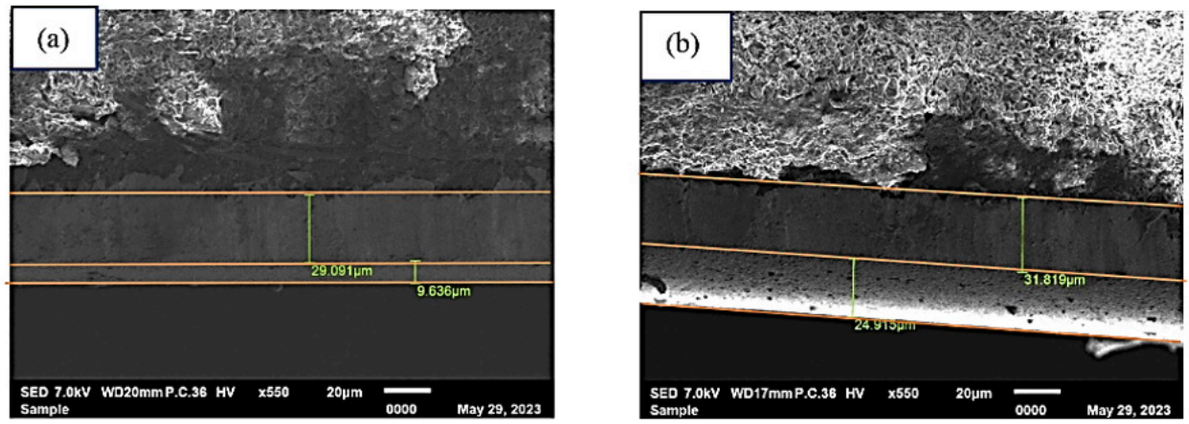

FIGURE 9. SEM characterization of copper oxide layer thickness that was oxidized by (a) 24 hours and (b) 48 hours by 5M NaOH

2. ZINC OXIDE

The zinc structure formed in Figure 10 shows the layer-by-layer flat platelet structure which yielding the same result as Alias & Mohamad (2015). However, the time to electrodeposit was different, taking only 30 minutes compared to 1 hour for Alias & Mohamad (2015). This allows time consumption to be minimized.

Figure 11 shows the structure of zinc oxide formed after chemical bath deposition technique. It was similar to the result obtained by Jyoti et al. 2013, but the particles were more uniform and spherical due to the high deposition temperature applied. According to Jyoti et al. 2013, deposition temperature affects the size of the particles, changing the shape and increasing the size.

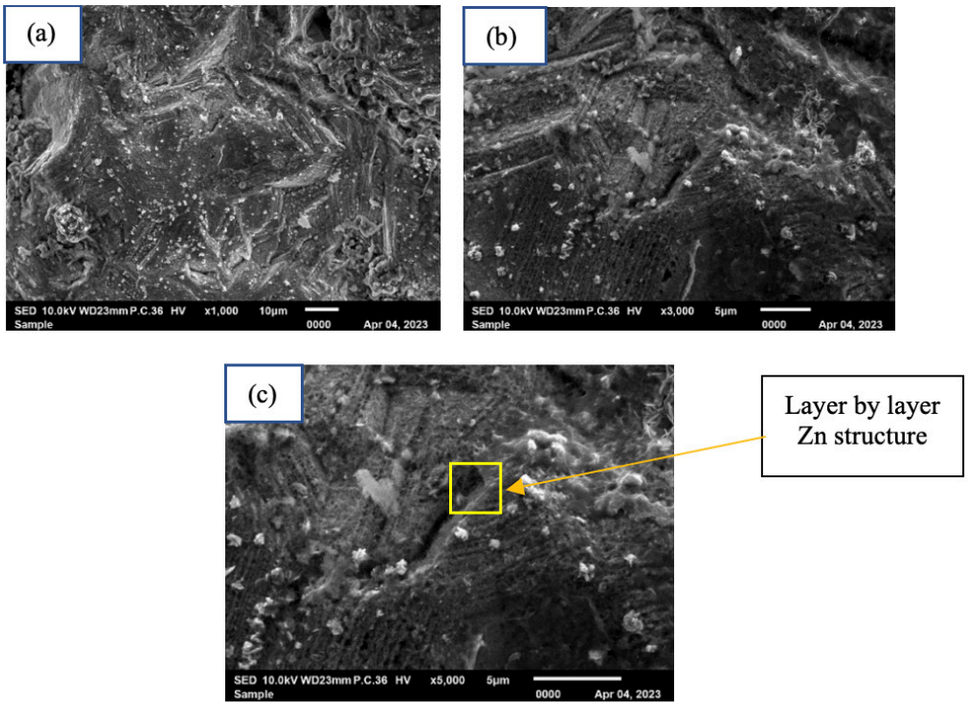

FIGURE 10. SEM characterization of zinc deposited by electrodeposition with magnification of a) x1000, b) x3000, and c) x5000 respectively

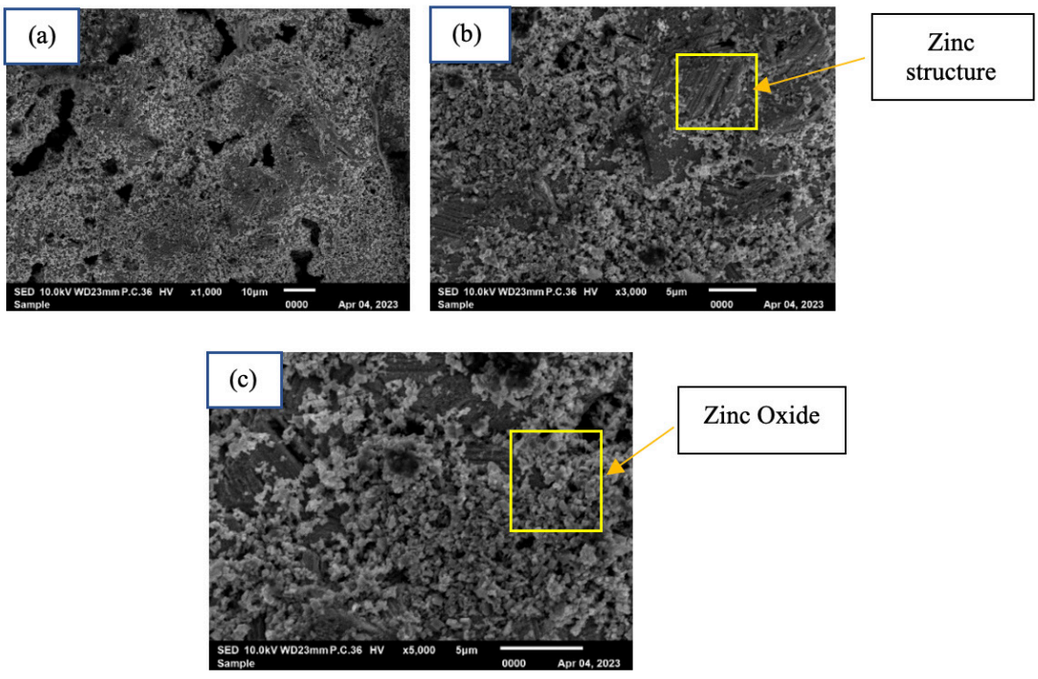

FIGURE 11. SEM characterization of zinc oxide deposited by electrodeposition with magnification of a) x1000, b) x3000, and c) x5000 respectively

X-RAY DIFFRACTION (XRD) ANALYSIS

Figure 12 shows that the CuO peak for CuO layer that has been oxidized by 5M NaOH for 24 hours can clearly be seen compared to CuO that have been oxidized by 3M and 4M NaOH. The XRD pattern shows prominent reflections along (110), (-111), (111) planes respectively at 2θ=32.55˚, 35.69˚, 38.733˚ for CuO and (111), (200), and (220) for Cu are seen.

Figure 13 shows that CuO which oxidized for 48 hours has higher peaks than CuO which oxidized for 24 hours. This suggests that the greater oxidation period resulted in a higher degree of crystallinity (crystallite size = 6nm) or a bigger volume percentage of the CuO phase according to Valladares et. al 2012. Cu, Zn, and ZnO are the elements that occur in ZnO XRD pattern. In this example, the peaks associated with zinc (Zn) would come from the electrodeposited Zn layer, whereas the peaks related with copper (Cu) would come from the underlying copper substrate. The XRD patterns shows prominent reflections along (110), (002), and (101) planes which indicates that ZnO thin film were successfully deposited on the substrates as can be seen in the SEM images in Figure 11.

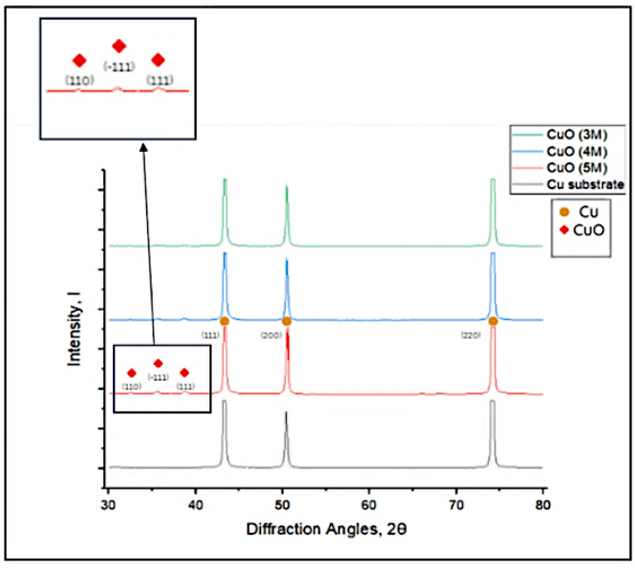

FIGURE 12. XRD pattern of CuO oxidized by 3M, 4M, 5M NaOH for 24 hrs and copper PCB substrate

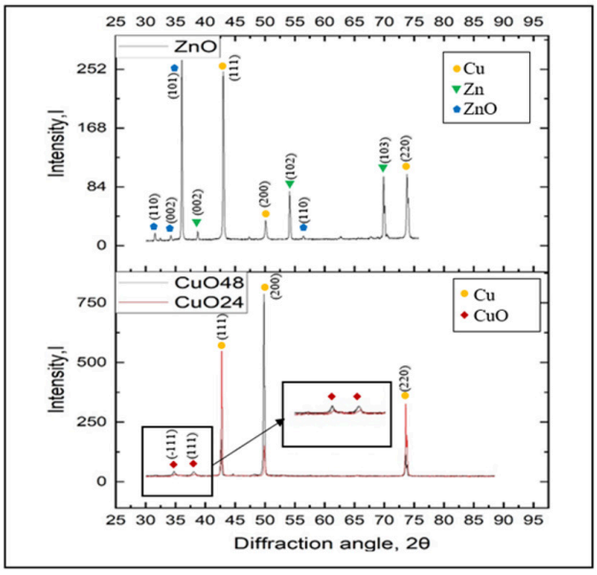

FIGURE 13. XRD pattern of ZnO layer and CuO oxidized by 5M NaOH for 24 and 48 hours

THERMOELECTRIC PROPERTIES ANALYSIS

TEMPERATURE GRADIENT AND VOLTAGE EXPERIMENT (SEEBECK PROPERTIES)

CuO and ZnO layer were tested independently. The temperature gradient applied to each sample were varied from 3°C, 6°C and 10°C consequently. The temperature gradient versus time graph was plotted in Figure 14. The graph shows the temperature increases step by step before it become constant and achieve stable temperature. From the Figure 15, CuO which was oxidized by 48 hours yield slightly higher Seebeck voltage compared to CuO which was oxidized by 24 hours. According to Walia et al. 2013, thicker CuO layer can yield higher Seebeck voltage output compared to thin CuO layer.

The Seebeck coefficient can be calculated from the Seebeck voltage versus temperature difference graph in Figure 15. The average Seebeck coefficient of both p-type CuO and n-type ZnO was summarized in Table 1. n-type ZnO has a negative Seebeck coefficient, which implies that when a temperature gradient is placed across the material, it produces a negative voltage while p- type CuO has a positive Seebeck coefficient. During 0°C, Seebeck voltage for p-type CuO and n-type ZnO supposedly equal to zero, but there was parasite voltage during the measurement. Parasite voltage may occur due to contact resistance, and it is best to use low-resistance connections and appropriate contact procedures to reduce this impact.

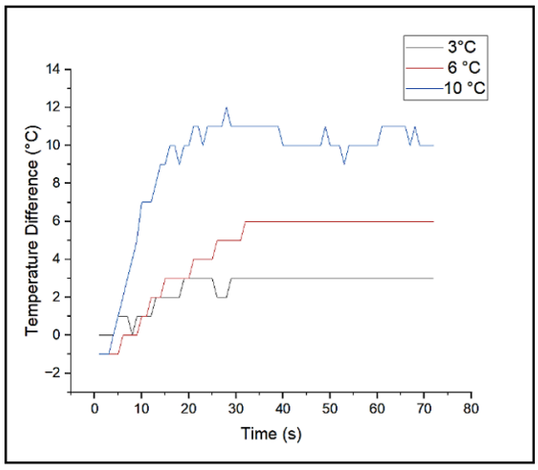

FIGURE 14. Temperature difference versus time graph. Seebeck voltage versus time graph

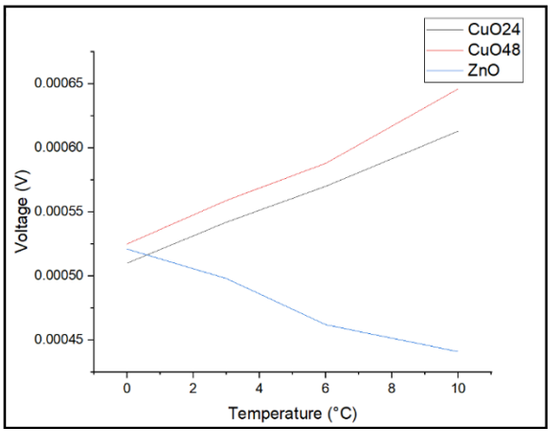

FIGURE 15. Seebeck voltage versus temperature difference graph for both CuO and ZnO

TABLE 1. Average Seebeck coefficient for CuO oxidized for 24, 48 hours and ZnO.

	CuO (24h)	CuO (48h)	ZnO
Average Seebeck Coefficient (μV/K)	+10.224	+11.950	-8.283

CURRENT-VOLTAGE EXPERIMENT (ELECTRICAL CONDUCTIVITY)

The current-voltage experiment was conducted to measure the electrical conductivity of both CuO and ZnO independently. No temperature gradient was applied and the probe placement was the same as the temperature gradient and voltage experiment. Electrical conductivity of the sample can be calculated based on formula below:

$$\sigma = 1/\rho \quad (2)$$

$$\rho = RA/L \quad (3)$$

$$R = 1/m \quad (4)$$

σ = Electrical conductivity (S/m)
ρ = Resistivity of the material (Ω.m)
A = Cross-sectional area of the sample (cm^2)
L = Length of the sample (m)
R = Resistance of the sample (Ω)
m = Gradient of the I-V graph

Figure 16 shows an I-V graph of each sample and resistance can be obtained from its gradient. Table 4.2 summarized resistance, resistivity, and electrical conductivity for both CuO and ZnO. CuO oxidized by 48 hours yields high electrical conductivity compared to CuO oxidized by 24 hours. A longer oxidation period enables a more thorough conversion of Cu to CuO, increasing the crystallinity of the CuO structure. Compared to amorphous or less structured structures, crystalline materials typically display superior electrical conductivity (Valladares et al. 2012). ZnO yields higher electrical conductivity due to its wider bandgap, which makes it easier for charge carriers to pass through the material. CuO has a lower conductivity due to a greater energy barrier for charge carrier transport.

TABLE 2. Summarization of resistance, resistivity, and electrical conductivity of the sample

Sample	R (Ω)	P (Ω.m)	σ (S/m)
CuO (24h)	5.760	0.068	14.706
CuO (48h)	4.384	0.052	19.231
ZnO	3.293	0.030	33.333

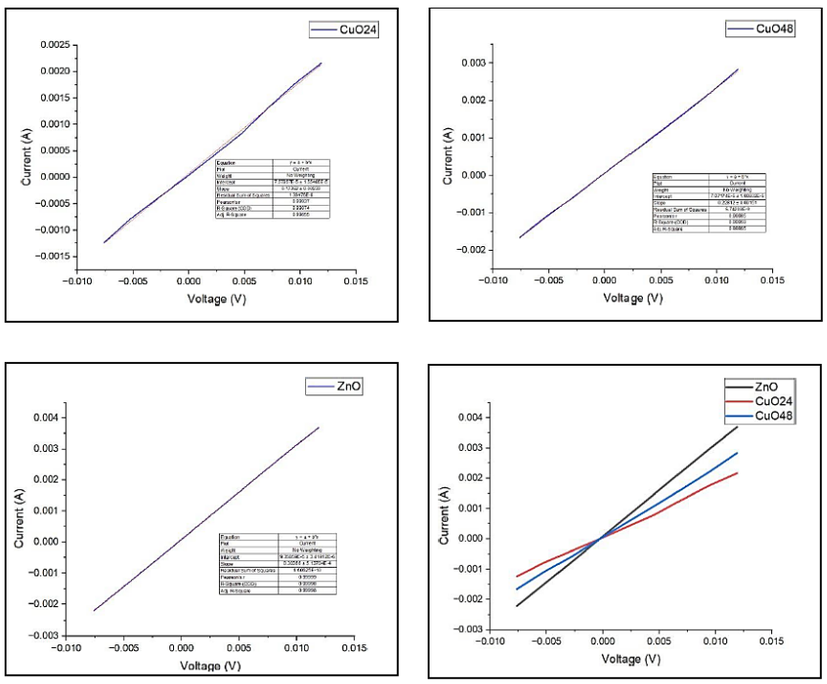

FIGURE 16. I-V graph for sample (a) CuO oxidized for 24 hours (b) CuO oxidized for 48 hours and (c) ZnO and (d) I-V graph for CuO oxidized by 24 and 48 hours and ZnO

THERMOELECTRIC POWER FACTOR

TPF is a key parameter used to evaluate the performance of a material for thermoelectric applications. TPF of the sample can be calculated based on the formula below:

$$PF = S^2\sigma \quad (5)$$

PF = Power Factor (μW/K2 m)
S = Seebeck coefficient of the sample (μV/K)
σ = Electrical conductivity of the sample (S/m)

The thermoelectric power factor for CuO oxidized by 24 and 48 hours was 1.537 and 2.746 n respectively. According to the equation 4, the Seebeck coefficient and electrical conductivity obtained an impact on its PF. CuO oxidized for 24 hours has lower S and σ values than CuO oxidized for 48 hours, therefore its PF value will likewise be lower. In contrast to Zappa et al. 2014 study, the PFs for CuO and ZnO obtained from this experiment were lower due to the difference in deposition temperature and fabrication method. The structure morphology was strongly influenced by the growth temperature, with samples generated at the greatest temperature exhibiting larger-sized nanostructures than samples grown at lower temperatures.

TABLE 3. Summarization of Seebeck coefficients, electrical conductivity, and power factor of both CuO and ZnO.

	S (μV/K)	σ (S/m)	PF (n)
CuO (24h)	+10.224	14.706	1.537
CuO (48h)	+11.950	19.231	2.746
ZnO	-8.283	33.670	2.310

CONCLUSION

The CuO-ZnO semiconductor was successfully fabricated by adopting simple and low-cost deposition procedures for each stage, beginning with p-type CuO semiconductor fabrication by alkaline vapour deposition and progressing to n-type ZnO semiconductor fabrication using electrodeposition and chemical bath deposition techniques. The morphology obtained from SEM images were similar to previous research, and XRD test was carried out to study the composition present in the sample. The seebeck effect on both semiconductors was studied by measuring the voltage output when a temperature difference is applied to the sample. It can be concluded that p-type CuO yield positive Seebeck coefficient while n-type (ZnO) yield negative Seebeck coefficient. The electrical conductivity of the p-type CuO and n-type ZnO semiconductor can be determined from the I-V graph obtained, which n-type ZnO produced higher electrical conductivity compared to p-type CuO. The thermoelectric power factor can be calculated by using seebeck coefficient and electrical conductivity obtained. The results obtained are smaller compared to the literature review due to the different fabrication methods and low fabrication temperature used during fabrication process. The optimum results were achieved with n-type ZnO, which had a PF value of 2.310 nW/K^2 m, σ value of 33.670 S/m and S value of -8.283 μV/K. While p-type CuO which underwent 48 hours of oxidation had the best PF value of 2.746 nW/K^2 m, σ value of 19.231 S/m and S value of +11.950 μV/K.

ACKNOWLEDGEMENT

The authors would like to acknowledge International Islamic University Malaysia for supporting the study under Grant IUMP-SRCG22-021-0021.

DECLARATION OF COMPETING INTEREST

None.

REFERENCES

Alias, N., & Mohamad, A. A. 2015. Morphology study of electrodeposited zinc from zinc sulfate solutions as anode for zinc-air and zinc-carbon batteries. *Journal of King Saud University - Engineering Sciences* 27(1): 43–48

Auberlet, J.-M., Rosey, F., Anceaux, F., Aubin, S., Briand, P., Pacaux, M.-P., & Plainchault, P. 2012. The impact of perceptual treatments on driver's behavior: from driving simulator studies to field tests-first results. *Accident Analysis and Prevention* 45(2): 91-98.

Jyoti, M., Vijay, D., & Radha, S. 2013. To study the role of temperature and sodium hydroxide concentration in the synthesis of zinc oxide nanoparticles. *International Journal of Scientific and Research Publications* 3(11): 2250-3153.

Nkrumah, I., Ampong, F. K., Kwakye-Awuah, B., Nkum, R. K., & Boakye, F. 2013. Synthesis and characterization of ZnO thin films deposited by chemical bath technique. *International Journal of Research in Engineering and Technology* 2(12).

Shuai, J., Mao, J., Song, S., Zhang, Q., Chen, G., & Ren, Z. 2017. Recent progress and future challenges on thermoelectric Zintl materials. *Materials Today Physics* 1: 74-95.

Soejima, T., Takada, K., & Ito, S. 2013. Alkaline vapor oxidation synthesis and electrocatalytic activity toward glucose oxidation of CuO/ZnO composite nanoarrays. *Applied Surface Science* 277: 192–200.

Su, L., & Gan, Y. X. 2011. Advances in thermoelectric energy conversion nanocomposites. *Advances in Composite Materials for Medicine and Nanotechnology*, 119.

Sulaiman, S., Sudin, I., Al-Naib, U. M. B., & Omar, M. F. 2022. Review of the nanostructuring and doping strategies for high-performance ZnO thermoelectric materials. *Crystals* 12(8): 1076.

Valladares, L. D. L. S., Salinas, D. H., Dominguez, A. B., Najarro, D. A., Khondaker, S. I., Mitrelias, T., & Majima, Y. 2012. Crystallization and electrical resistivity of Cu_2O and CuO obtained by thermal oxidation of Cu thin films on SiO_2/Si substrates. *Thin Solid Films* 520(20): 6368-6374.

Walia, S., Balendhran, S., Nili, H., Zhuiykov, S., Rosengarten, G., Wang, Q. H., & Kalantar-zadeh, K. 2013. Transition metal oxides–Thermoelectric properties. *Progress in Materials Science* 58(8): 1443-1489.

Xiong, D. B., Okamoto, N. L., & Inui, H. 2013. Enhanced thermoelectric figure of merit in p-type Ag-doped ZnSb nanostructured with Ag3Sb. *Scripta Materialia* 69(5): 397-400.

Zappa, D., Dalola, S., Faglia, G., Comini, E., Ferroni, M., Soldano, C., Ferrari, V., & Sberveglieri, G. 2014. Integration of ZnO and CuO nanowires into a thermoelectric module. *Beilstein Journal of Nanotechnology* 5: 927–936.